

Strong gyrotropy in a chiral toroidal medium

N. Papasimakis, V. A. Fedotov, K. Marinov, and N. I. Zheludev
*Optoelectronics Research Centre, University of Southampton, SO17 1BJ, UK**

A. D. Boardman
Institute for Materials Research, University of Salford, M5 4WT, UK
 (Dated: June 3, 2021)

In this letter, we present the first experimental study of a new chiral metamaterial consisting of toroidal wire windings. We show that the metamaterial exhibits three bands of circular dichroism in the GHz range. We discuss the response of the structure in terms of multipole moments, including the (magnetic) toroidal dipole moment.

Toroidal, doughnut-shaped structures are ubiquitous in nature, appearing on scales which range from the sub-atomic [1, 2] to the astronomical [3]. On the molecular level, the torus shape is preferred by numerous biological and chemical macromolecules, such as DNA condensates [4], proteins [5] and oligosaccharides [6], to name just a few. Toroidal symmetries are also encountered frequently in solid-state systems including carbon nanotubes [7] and ferroelectrics [8, 9]. Although the behavior of such systems has been studied extensively, their interaction with electromagnetic radiation is not well understood. Indeed, within the framework of classical electrodynamics, unusual phenomena associated with violation of Lorentz reciprocity [10] and non-radiating configurations [11] have been predicted for toroidal structures and their interactions. Nevertheless, such phenomena are usually weak [12, 13] and, therefore, experimental investigations are rare. In this letter, we study a new artificial chiral medium, originally suggested in [14], consisting of an array of toroidal wire windings in a metamaterial configuration. We show that such a metamaterial exhibits strong gyrotropic response which is attributed to different terms of its multipole expansion.

In contrast to artificial gyrotropic media, where handedness is usually associated with the direction of a "twist vector" following a cork-screw law along the helicity axis, the situation is more complicated when the structure possesses toroidal symmetry. Here, the twist vector rotates along the torus, and therefore a corresponding direction can not be defined. However, although no helicity axis exists, the structure has two well-defined enantiomeric forms, corresponding to different directions of the winding (see Fig. 1a). Based on this concept, we manufactured a chiral toroidal metamaterial with a unit cell consisting of four connected square loops that were formed by horizontal and vertical copper wire segments (see Fig. 1b). The resulting windings were embedded in dielectric bars with permittivity $\epsilon = 4.5 - 0.081i$. The size of the unit cell was $15 \times 15 \text{ mm}$ rendering the metamaterial non-diffracting up to 20 GHz . Transmission experiments were performed at normal incidence, from 2 to 14 GHz , in an anechoic chamber using two broad-

band horn antennas (Schwarzbeck M. E. model BBHA 9120D). The transmission spectra were recorded with a vector network analyzer.

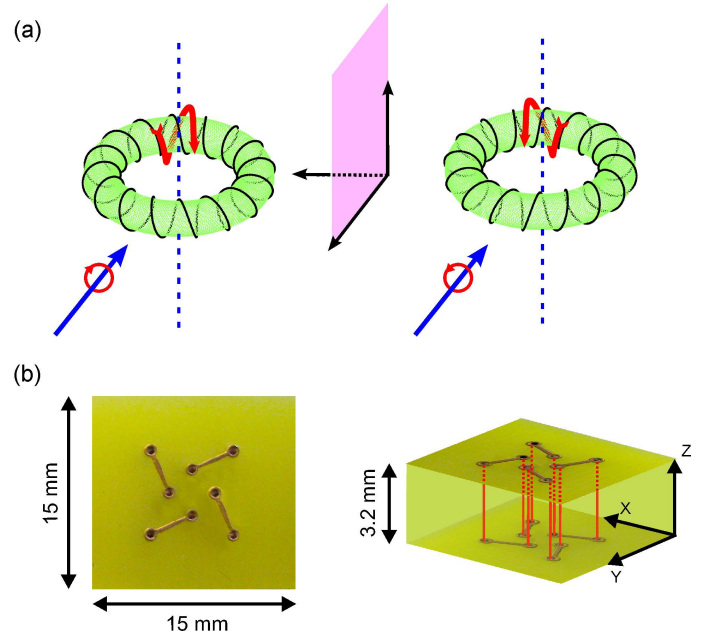


FIG. 1: (a) Left- and right-handed form of a chiral toroidal winding. The electromagnetic response of the structure is determined by the handedness of the winding and that of the incident wave. (b) Top and side view of the fabricated toroidal metamaterial unit cell.

The intensity and phase of the structure's response to right and left circularly polarized light are presented in Figs. 2a and 2b, respectively. As it can be seen in Fig. 2a, experimental results (solid line) are in good agreement with finite element numerical simulations (solid circles). Two resonant bands of strong circular dichroism can be distinguished at around 4.5 and 10 GHz , where the corresponding transmission ratio for orthogonal circularly polarized states reaches 5 and 15 dB with bandwidth (FWHM) 370 MHz and 1.6 GHz , respectively. Moreover, while the rejected polarization state experiences high losses, the orthogonal polarization state propagates through the structure almost unaffected. This is also ev-

ident from the behavior of the phase delay presented in Fig. 2b. In addition, the rejected polarization state corresponds to a backward wave, while the other to a normal propagating wave, since they both have the same sign of phase velocity, but different signs of group velocity. This can be considered as a plausible indication for the presence of negative refraction [15]. Finally, a third band of circular dichroism can also be seen at around 7.5 GHz. In this case, however, the dichroism is weaker, while both polarization states experience significant losses.

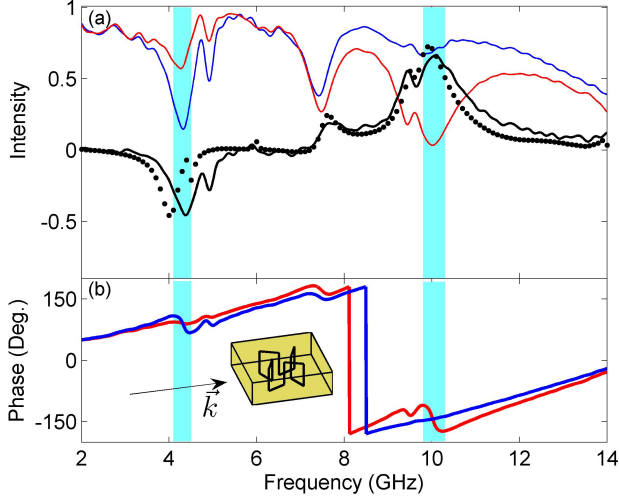


FIG. 2: (a) Transmitted intensity for right (blue) and left (red) circularly polarized light. The circular dichroism is represented by the solid black curve (experimental) and the black solid circles (numerical). The position of the dichroism resonances is marked by the blue panels. (b) Phase delay for right (blue) and left (red) circularly polarized light. Inset: Unit cell of the studied metamaterial and direction of wave propagation.

The observed resonances are of geometrical origin and their frequency position is controlled by the ratio of the total wire length in the metamaterial unit cell over the wavelength of the incident wave, while the presence of the dielectric has to be taken also into account. In general, geometrical resonances will occur whenever, the total wire length equals an integer number of half-wavelengths. However, due to the symmetry of the structure only an even number of nodes is allowed. Therefore, resonances will occur whenever the wire length equals an integer multiple of the excitation wavelength (even number of nodes). At these resonances, the intensity of interaction is very different for left and right circular polarization. This is illustrated in Figs. 3a & 3b, where energy density maps and power flow lines (following the Poynting vector) are shown. While one polarization interacts strongly with the structure (Fig. 3a) the orthogonal circular polarization propagates almost unaffected. This behavior is also demonstrated in Figs. 3b and 3c, where the real

part of the current intensity along the wire winding is plotted for the case of the low frequency (4 GHz) and high frequency (10 GHz) resonances. Although the current configuration is very similar for both polarizations, resembling standing waves with four (4 GHz) and six nodes (10 GHz), its intensity is significantly different which leads to the observed dichroism resonances.

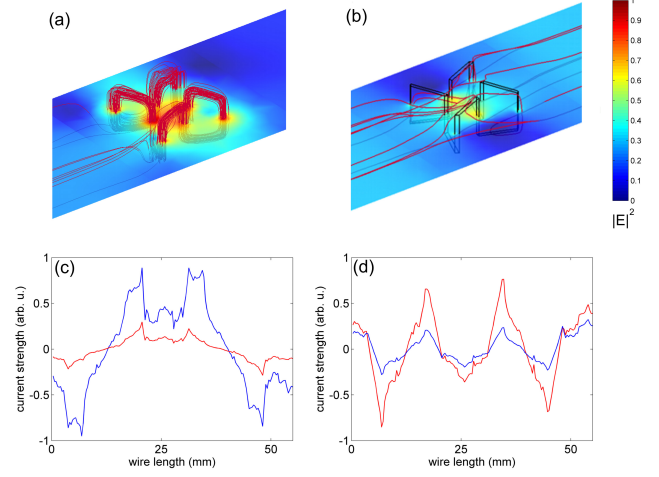


FIG. 3: Finite element simulations of toroidal metamaterial. (a) and (b) show electric density (color maps) and powerflow lines at the 4 GHz resonance for right and left circularly polarized incident wave, respectively. (c) and (d) present induced current configuration on the wire winding for right (red) and left (blue) circularly polarized light, at the 4 GHz and 10 GHz resonances, respectively.

In the framework of multipole theory, the observed gyrotropy arises from the coupling of the electric and magnetic dipole moments, but can also include a contribution from the electric quadrupole moment, since the metamaterial is anisotropic [17, 18]. In order to further investigate the metamaterial's response, we calculate the induced multipole moments [19] under plane wave illumination. The multipole moments have been calculated by the following relations:

$$\begin{aligned} \text{electric dipole :} \quad p_i &= \frac{1}{i\omega} \int J_i dV \\ \text{magnetic dipole :} \quad m_i &= \frac{1}{2} \int (\vec{r} \times \vec{J})_i dV \\ \text{electric quadrupole :} \quad Q_{ij} &= \frac{1}{i\omega} \int (r_i J_j + J_i r_j) dV, \end{aligned}$$

where $i, j = x, y, z$ and compared their strength in terms of radiated power:

$$\begin{aligned} \text{el. dipole radiation :} \quad P_p &= \frac{\omega^4 \mu_0}{12\pi c} |\vec{p}|^2 \\ \text{m. dipole radiation :} \quad P_m &= \frac{\omega^4 \mu_0}{12\pi c^3} |\vec{m}|^2 \\ \text{el. quadrupole radiation :} \quad P_Q &= \frac{\omega^6 \mu_0}{160\pi c^3} \sum |Q_{ij}|^2, \end{aligned}$$

as presented in Fig. 4. As expected, the electric dipole moment dominates the response of the system at all frequencies, while all multipole moments resonate together at the 4 GHz and 10 GHz circular dichroism bands. More concisely, at the low frequency resonance, the magnetic dipole is much stronger than the electric quadrupole, indicating that the main contribution to chirality comes from the electric dipole-magnetic dipole coupling. This is also supported by the fact that these moments are almost collinear as shown in the corresponding inset of Fig. 4. Similar situation arises also at the high frequency dichroism band (10 GHz). However, at the weaker 7 GHz resonance, the electric quadrupole presents a pronounced resonance, while the magnetic dipole moment is weaker. This suggests that the weak dichroism at this resonance is a result of electric dipole - electric quadrupole coupling. Although ideally the electric dipole moment should also be at a minimum, the dominant contribution is still coming from the latter, as a result of the finite size of the structure.

In addition, we include in our analysis the (magnetic) toroidal dipole moment [1]. Indeed, it has been suggested that the complete multipole expansion requires the inclusion of toroidal moments along with the electric and magnetic ones [21]. While usually these moments can be neglected, this is not true for structures comparable to the wavelength or structures of toroidal symmetry [21], as the one considered here. In fact, the toroidal moment is known to result in magneto-electric coupling [22], since it enters the multipole expansion in exactly the same way as the electric moments [21]. Therefore one can expect that coupling between toroidal and magnetic moments would lead to optical activity and the question of a toroidal contribution to the observed chirality arises. In order to quantify the toroidal response of the metamaterial, we calculate its toroidal moment by the formula, $\vec{\tau} = \int [(\vec{r} \cdot \vec{j})\vec{r} - r^2\vec{j}]d^3r$ and present in Fig. 4 the corresponding radiated power $P_T = \frac{\omega^6 \mu_0}{12\pi c^5} |\vec{T}|^2$ [19]. At most frequencies the toroidal moment is comparable with the electric quadrupole moment, which suggests that the toroidal contribution to the metamaterial response is in general non-negligible. However, as it can be seen from the radiated powers, its contribution in the gyrotropy is secondary, since the electric and magnetic dipole/electric quadrupole moments are much stronger at the dichroism resonances. Nevertheless, a much stronger toroidal response is expected at lower frequencies, where electric multipole moments vanish and we intend to study this regime in the near future.

In conclusion, we present a first experimental investigation of a new type of chiral metamaterials, which possesses toroidal symmetry. The studied metamaterial shows strong circular dichroism in the GHz frequency range as a result of geometrical resonances. The gyrotropic response of the structure can be explained in

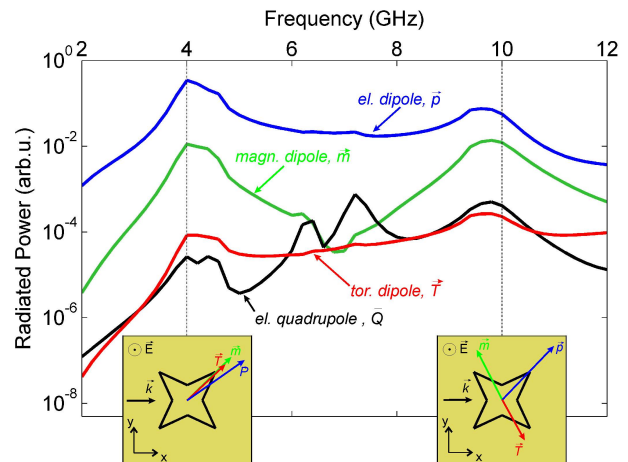


FIG. 4: Radiated power from the different multipole moments of the (numerically simulated) current configuration on the wire windings, normalized to the incident power. Insets: Orientation in the x-y plane of dipole moments at the frequencies marked by the corresponding dashed lines. In both cases, the z-component of the moments is much smaller than the x and y components.

terms of electric and magnetic dipole as well as electric quadrupole moments. Finally, we discussed the toroidal response of the system and showed that at specific frequencies it can be of magnetic dipole/electric quadrupole order.

The authors would like to acknowledge the financial support of the Engineering and Physical Sciences Research Council, UK.

References

-
- * Electronic address: N.Papasimakis@soton.ac.uk
 - [1] Zel'dovich, Ya. B., Zh. Eksp. Teor. Fiz. **6**, 1184 (1958).
 - [2] V. M. Dubovik, A. A. Cheshkov, Phys. Part. Nucl. **5**, 791 (1974).
 - [3] J. S. Mainstone, Nat. **215**, 1048 (1967).
 - [4] N. V. Hud and I. D. Vifan, Annu. Rev. Biophys. Biomol. Struct. **34**, 295-318 (2005).
 - [5] M. M. Hingorani and M. O'Donnell, Nat Rev. Mol. Cell Biol. **1**, 22-30 (2000).
 - [6] W. Saenger, J. Jacob, K. Gessler, T. Steiner, D. Hoffmann, H. Sanbe, K. Koizumi, S. M. Smith, and T. Takaha, Chem. Rev. **98**, 1787-1802 (1998).
 - [7] J. Lium H. Dai, J. H. Hafner, D. T. Colbert, R. E. Smalley, S. J. Tans, and C. Dekker, Nature **385**, 780-781 (1997).

- [8] A. A. Gorbatsevich and Y. V. Kopaev, *Ferroelectrics* **161**, 321-324 (1994).
- [9] I. I. Naumov, L. Bellaiche and H. X. Fu, *Nature* **432**, 737-740 (2004).
- [10] G. N. Afanasiev, *J. Phys. D* **34**, 539-559 (2001).
- [11] G. N. Afanasiev and V. M. Dubovik, *Phys. Part. Nucl.* **29**, 366 (1998).
- [12] Sawada K and Nagaosa N 2005 *Phys. Rev. Lett.* **95** 237402
- [13] V. A. Fedotov, K. Marinov, A. D. Boardman and N. I. Zheludev, *New J. Phys.* **9**, 95 (2006).
- [14] K. Marinov, A. D. Boardman, V. A. Fedotov, and N. I. Zheludev, *New J. Phys.* **9**, 324 (2007).
- [15] J. B. Pendry, *Science* **306**, 1353 (2004).
- [16] R. E. Raab and O. L. de Lange, *Multipole Theory in Electromagnetism* (Oxford, 2005).
- [17] A. D. Buckingham and M. B. Dunn, *J. Chemical Soc. A*, 1988 (1971).
- [18] I. P. Theron and J. H. Cloete, *IEEE Trans. Antennas Propagat.* **44**, 1451 (1996).
- [19] C. Vrejoiu, *J. Phys. A: Math. Gen.* **35**, 9911 (2002).
- [20] Similar results were obtained under excitation with the orthogonal polarization state (y axis of Fig. 1b).
- [21] V. M. Dubovik and V. V. Tugushev, *Phys. Rep.* **187**, 145 (1990).
- [22] M. Fiebig, *J. Phys. D* **38**, R123 (2005).